Use of contrast-enhanced magnetic resonance imaging of the pelvis to describe changes at different anatomic sites which are potentially specific for polymyalgia rheumatica

M. Fruth[1], B. Buehring[2], X. Baraliakos[2], J. Braun[2]

[1]Radiologie Herne am Rheumazentrum Ruhrgebiet, Herne, Germany
[2]Rheumazentrum Ruhrgebiet, Herne, Germany.

Martin Fruth, MD
Bjoern Buehring, MD
Xenofon Baraliakos, MD
Jürgen Braun, MD

Please address correspondence to:
Dr Martin Fruth,
Radiologie Herne am
Rheumazentrum Ruhrgebiet,
Claudiusstraße 45,
44649 Herne, Germany.
E-mail: fruth@radiologieherne.de

Received on June 24, 2018; accepted in revised form on September 7, 2018.

Clin Exp Rheumatol 2018; 36 (Suppl. 114): S86-95.

Key words: magnetic resonance imaging, inflammation, polymyalgia rheumatica

Competing interests: none declared.

ABSTRACT

Objective. *To identify inflammatory pelvic structures of patients with polymyalgia rheumatica (PMR) by magnetic resonance imaging (MRI) in detail, searching for a disease-specific pattern.*

Methods. *A total of 40 contrast-enhanced pelvic MRIs of patients with a clinical diagnosis of PMR was reviewed by an experienced musculoskeletal radiologist who assessed all abnormalities semi-quantitatively, based on a predefined scoring system.*

Results. *The median (25th/75th percentiles) age of patients was 67 (55/73) years, median symptom duration 13 (6/22) weeks, 55% female, median CRP 1.9 (0.7/4) mg/dl, median ESR 30/1h (17/43). Ten patients were diagnosed with rheumatoid arthritis (25%), in addition to their leading polymyalgic symptom. Multi-locular, mostly bilateral, peritendinous enhancement of pelvic girdle tendons was found to be the hallmark of PMR in all patients. Low-grade hip synovitis was also detected frequently. In all cases, ≥4 extracapsular tendinous sites were bilaterally affected. Besides involvement of the common ischiocrural tendon and the glutaeus medius and minimus tendon (present in all cases), an enhancement of the proximal rectus femoris origin was observed in 100% and of the adductor muscles at the inferior medial pubic bone in 90% of cases. The observed MRI pattern patho-anatomically suggests inflammation of the external peritendineum.*

Conclusion. *The uniformity of the observed pelvic inflammatory pattern detected by contrast-enhanced MRI in PMR patients suggests that it may become relevant for diagnostic purposes. The bilateral involvement of at least 4 extracapsular sites (including the origins of proximal rectus femoris or adductorial muscles) appears to be characteristic of PMR.*

Introduction

Patients suffering from polymyalgia rheumatica (PMR) usually complain about pain in the pelvic girdle, a frequent and characteristic, however non-specific, symptom of this rather common disease (1). The neck and shoulder region is also regularly involved (2). The differential diagnosis of PMR which covers not only giant cell arteritis (GCA), but also other vasculitides and autoimmune diseases, infections and malignancy, can be challenging, since "gold standard" specific imaging findings and laboratory tests are not available (3, 4). Of course, markers of inflammation such as C-reactive protein (CRP) and erythrocyte sedimentation rate (ESR) are usually elevated, but this finding is seen in most inflammatory rheumatic diseases. Thus, a diagnosis of PMR is usually based on clinical judgement and the exclusion of other diagnoses. For confirmation of the diagnosis, a therapeutic trial of prednisolone is generally initiated (5).

International recommendations for the performance of imaging procedures in PMR and GCA have recently been published (6). Synovial inflammation, mainly in the bursae around the shoulder and the pelvic girdle, has been described in PMR patients using ultrasound (5, 6). However, these findings also lack specificity, due to the high incidence of degenerative and stress-related periarticular changes in this region seen in this age group (7). A metaanalysis suggested that the most helpful ultrasound feature for PMR diagnosis is subacromial-subdeltoid bursitis – even though interpretation is limited by study heterogeneity and methodological issues, including variability in blinding and potential bias due to the different study designs (7).

On the other hand, with increasing use of PET-CT for non-oncological indica-

Table I. Overview of sequence parameters used.

	TR [ms]	TE [ms]	TI [ms]	Fatsaturation	FOV [mm]	Matrix	slice thickness [mm]/gap	Gd-contrast
Siemens Aera 1,5T								
T1w TSE coronal	511	10			400x400	320x320	6/20%	
T1w TSE transversal	526	13			400x250	240x384	6/20%	
T2w TIRM coronal	3550	56	160	inversion	400x400	320x320	6/20%	
T2w TIRM transversal	4400	59	160	inversion	400x250	384x240	6/20%	
T1w TSE FS coronal	477	8,3		spectral	400x400	320x320	6/20%	yes
T1w TSE FS transversal	476	11		spectral	400x250	200x320	6/20%	yes
Siemens Skyra 3,0T								
T1w TSE coronal	550	10			380x380	448x448	4/20%	
T1w TSE transversal	550	11			350x262,5	448x336	5/20%	
T2w TIRM coronal	5860	55	220	inversion	380x380	448x448	4/20%	
T2w TIRM transversal	5040	57	220	inversion	380x285	384x288	5/20%	
T1w TSE FS coronal	635	10		spectral	380x380	448x448	4/20%	yes
T1w TSE FS transversal	680	11		spectral	350x262,5	448x336	5/20%	yes
Siemens Avanto 1,5T								
T1w TSE coronal	490	12			400x400	768x768	5/30%	
T1w TSE transversal	583	10			370x307	786x636	6/20%	
T2w TIRM coronal	3500	57	140	inversion	400x400	320x320	5/30%	
T2w TIRM transversal	5100	63	160	inversion	370x296	320x256	6/20%	
T1w TSE FS coronal	565	12		spectral	400x400	640x640	5/30%	yes
T1w TSE FS transversal	590	11		spectral	370x300	256x208	6/20%	yes

tions, especially for cases with suspicion of GCA, inflammatory changes in the pelvic and the shoulder girdle as well as in other regions of the neck and the lumbar spine have been reported. In detail, extracapsular inflammation in and around tendons, entheses and bursae has been suspected in the pelvic girdle in several different locations (8-13). In more detail, involvement of the trochanteric and the ischiogluteal bursa, the praepubic insertion of the adductorial muscles, and the region around the acetabular rim has been described.

Comparable observations were made using contrast-enhanced (14) and non-contrast-enhanced magnetic resonance imaging (MRI) (15). These studies have highlighted the significance of extracapsular multi-locular inflammation beyond synovial inflammation of the hips as a hallmark of PMR in the pelvic girdle (8, 10, 14). The described inflammatory changes appear to affect tendinous insertional sites and pericapsular structures around the pelvic girdle – often bilaterally. Thus, it seems possible that the pathogenesis of PMR follows a characteristic pathoanatomical pattern of inflammation (16).

We have recognised these types of changes in MRI scans performed for

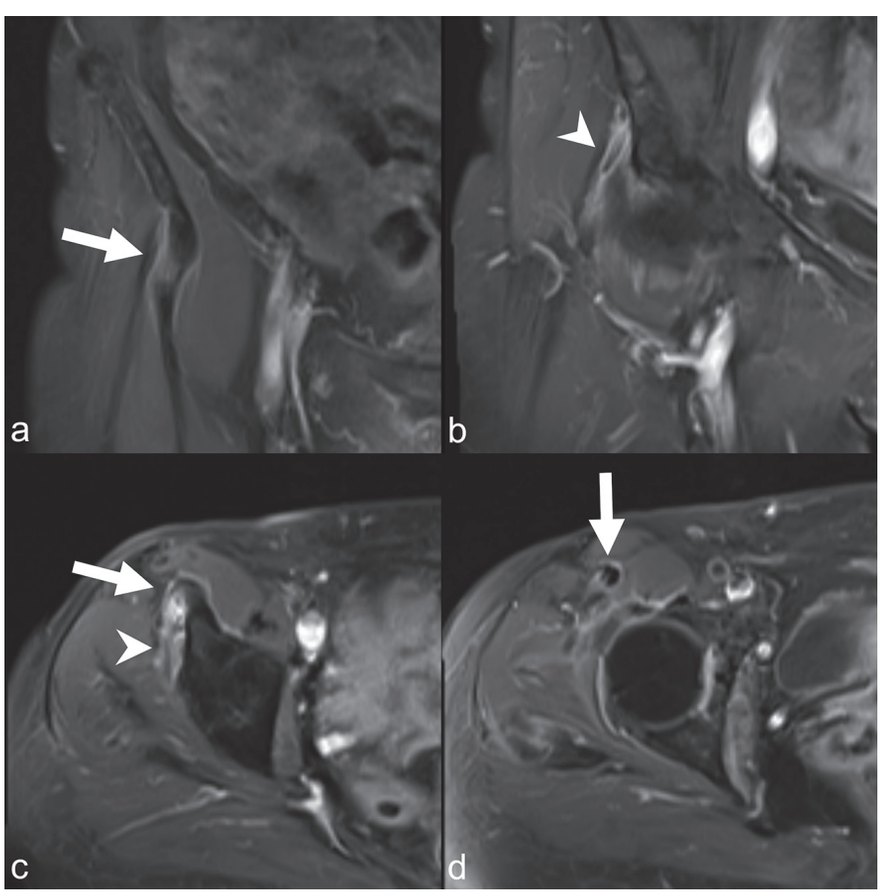

Fig. 1. Coronal (a/b) and transverse (c/d) ceT1w FS in the same patient. Peritendinous enhancement of straight (white arrow) and reflected (white arrow head) head of rectus femoris origins at anterior inferior iliac spine (a/c) and supraacetabular ridge (b). Peritendinous enhancement follows the tendon to the myotendinous junction (d).

differential diagnosis of PMR in our practice over the last years. Therefore, we performed a systematic retrospective study to describe changes seen in pelvic MRIs of well-characterised patients diagnosed with PMR on a clinical basis, independent of the MRI findings. Based on the good quality of the MRI technique, we are able to describe the location, distribution, and relative frequencies of involved sites in detail. Furthermore, we can illustrate the MRI-based patho-anatomy to provide better understanding of the pathophysiology of the disease. In addition, we describe a specific scoring system to increase the probability of correct diagnosis of PMR.

Methods

Patients

A total of 40 patients with PMR, including 10 patients with a concomitant diagnosis of rheumatoid arthritis (RA) and a PMR-like onset were identified using the clinical diagnoses and demographic data provided by the clinical information system (CIS) of our hospital – this implies that the diagnosis was made by a rheumatologist, which were connected to the images obtained from the radiologic information system (RIS) used in the clinic. Pelvic contrast enhanced MRIs of good quality

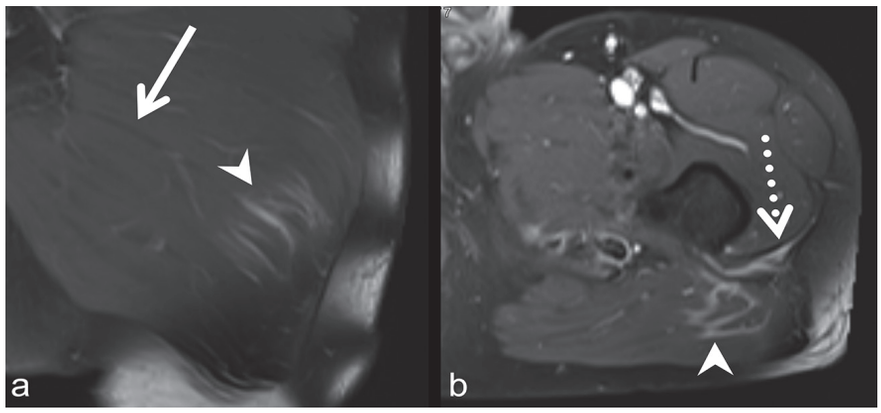

Fig. 2. Coronal and transverse ceT1w FS in the same patient. Linear enhancement of the intramuscular perimysium of inferolateral gluteus maximus (a/b, white arrow heads). More superomedial the perimysium is unaffected (**a**: white open arrow). Note the inflammation of lateral intermuscular septum and distal gluteus maximus insertion at gluteal tuberosity (**b**: dotted white arrow).

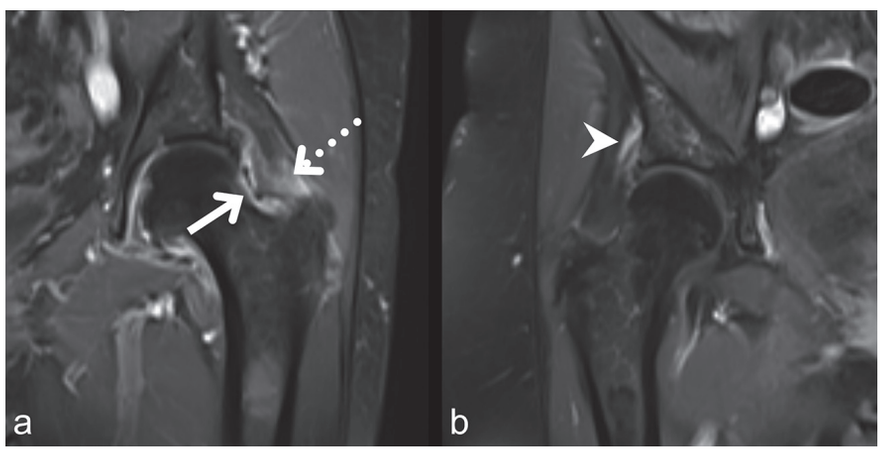

Fig. 3. Coronal ceT1w FS in two patients. Low grade synovitis (**a**: white open arrow) is clearly differentiable from capsular inflammation (dotted white arrow). In a different patient inflammation of reflected head rectus femoris (**b**: white arrow head) without any significant synovitis of hip joint.

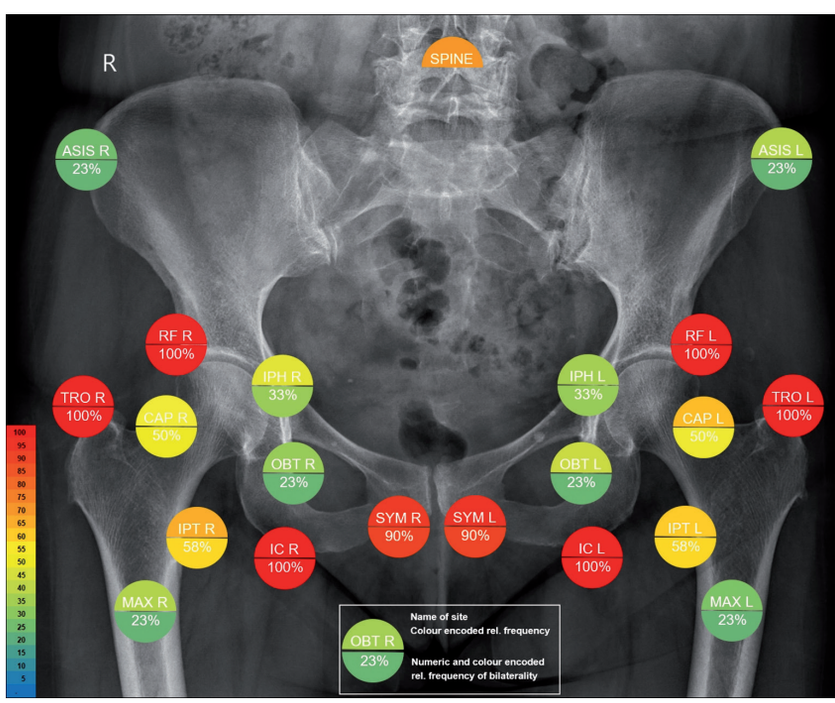

	Site	absolute	relative
SINGLE SITES	SPINE	28	70
	ASIS R	10	25
	ASIS L	15	38
	RF R	40	100
	RF L	40	100
	SYNO R	35	88
	SYNO L	35	88
	TRO R	40	100
	TRO L	40	100
	CAP R	21	53
	CAP L	25	63
	IPH R	19	48
	IPH L	14	35
	OBT R	13	33
	OBT L	17	43
	SYM R	37	93
	SYM L	38	95
	IPT R	26	65
	IPT L	24	60
	IC R	40	100
	IC L	40	100
	MAX R	15	38
	MAX L	11	28
BILATERALITY	ASIS	9	23
	RF	40	100
	SYNO	35	88
	TRO	40	100
	CAP	20	50
	IPH	13	33
	OBT	9	23
	SYM	36	90
	IPT	23	58
	IC	40	100
	MAX	9	23

Fig. 4. Distributional pattern of inflammation superimposed on pelvic x-ray. The upper semicircle represents colour encoded relative frequency of inflammation, the lower semicircle relative frequency of bilateral inflammation.

Table II. Tabular presentation of inflammation assessment in 40 cases, individual sum of affected sites and sum of bilateral affected sites are given. Detection of hip joint synovitis is listed but excluded in sums.

Case	Age	Gender	SPINE	ASIS R	ASIS L	RF R	RF L	SYNO R	SYNO L	TRO R	TRO L	CAP R	CAP L	IPH R	IPH L	OBT R	OBT L	SYM R	SYM L	IPT R	IPT L	IC R	IC L	MAX R	MAX L	Myositis	Osteitis	Sum all sites excl. SYNO	Number of sites bilateral
1	75	f	1	0	0	1	1	1	1	1	1	0	0	0	0	1	0	1	1	0	0	1	1	0	0	0	0	10	4
2	52	f	0	0	1	1	1	0	0	1	1	0	0	0	1	0	1	1	1	1	1	1	1	0	0	0	0	13	5
3	49	f	1	0	0	1	1	1	1	1	1	1	1	0	0	0	0	1	1	1	1	1	1	0	0	0	0	13	6
4	56	f	1	0	0	1	1	1	1	1	1	0	0	0	0	1	0	1	1	1	1	1	1	1	0	0	0	13	5
5	69	f	0	1	1	1	1	1	1	1	1	0	0	1	1	0	0	1	1	0	0	1	1	0	0	0	0	12	6
6	65	f	1	1	1	1	1	1	1	1	1	0	0	0	0	0	1	1	1	1	1	1	1	0	0	0	0	14	6
7	75	m	1	0	0	1	1	1	1	1	1	0	0	0	0	0	0	1	1	0	0	1	1	1	1	0	1	11	5
8	54	m	0	0	1	1	1	0	0	1	1	0	0	0	0	0	1	1	1	0	0	1	1	0	0	0	0	10	4
9	56	f	0	0	0	1	1	0	0	1	1	0	0	0	0	0	0	1	1	1	1	1	1	0	0	0	0	10	5
10	62	m	1	0	1	1	1	1	1	1	1	0	0	1	1	1	1	1	1	1	1	1	1	1	1	0	0	18	8
11	54	m	1	0	0	1	1	1	1	1	1	0	0	0	0	0	0	1	1	0	0	1	1	0	0	0	0	9	4
12	77	f	1	0	0	1	1	1	1	1	1	1	1	0	0	0	0	0	0	1	0	1	1	1	0	0	0	11	4
13	67	f	1	0	0	1	1	1	1	1	1	0	1	0	0	1	0	1	1	1	1	1	1	0	0	0	0	13	5
14	69	f	0	0	0	1	1	1	1	1	1	1	1	0	0	0	0	1	0	0	0	1	1	0	1	0	0	10	4
15	52	m	1	1	1	1	1	1	1	1	1	1	1	1	0	1	0	1	1	1	1	1	1	1	0	0	0	18	7
16	72	f	1	1	1	1	1	1	1	1	1	1	1	1	1	0	1	1	1	1	1	1	1	0	0	0	0	18	8
17	69	m	0	0	1	1	1	1	1	1	1	1	1	1	1	1	1	1	1	1	1	1	1	0	0	0	0	17	8
18	69	f	0	0	0	1	1	1	1	1	1	1	1	1	0	0	1	1	1	1	1	1	1	0	0	0	0	14	6
19	75	f	0	0	0	1	1	1	1	1	1	1	1	0	0	0	0	1	1	0	0	1	1	0	0	0	0	10	5
20	56	f	0	0	0	1	1	1	1	1	1	0	1	0	0	0	1	1	1	1	1	1	1	0	0	0	0	12	5
21	53	f	1	0	0	1	1	1	1	1	1	0	0	0	0	0	0	1	1	1	1	1	1	1	1	0	0	13	6
22	63	f	1	0	1	1	1	1	1	1	1	1	0	0	0	1	1	1	1	1	1	1	1	1	1	0	0	17	7
23	56	m	1	0	0	1	1	1	1	1	1	1	1	1	0	0	0	0	1	1	1	1	1	0	0	0	0	13	5
24	54	m	1	0	0	1	1	0	0	1	1	0	0	0	0	0	0	1	1	0	0	1	1	1	1	1	0	11	5
25	61	m	1	1	1	1	1	1	1	1	1	1	1	1	1	0	1	1	1	1	1	1	1	0	0	0	0	18	8
26	68	m	1	1	1	1	1	0	0	1	1	0	1	0	0	1	1	1	1	1	1	1	1	1	1	0	1	18	8
27	73	m	1	0	0	1	1	1	1	1	1	0	0	0	0	1	1	1	1	1	0	1	1	1	1	0	0	14	6
28	69	f	1	0	1	1	1	1	1	1	1	1	1	1	1	0	0	1	1	0	0	1	1	1	0	0	0	15	6
29	72	f	1	1	1	1	1	1	1	1	1	1	1	1	0	1	1	1	1	1	1	1	1	0	0	0	0	18	8
30	69	m	0	0	0	1	1	1	1	1	1	1	1	1	1	0	0	1	1	0	0	1	1	0	0	0	0	12	6
31	74	f	0	0	0	1	1	1	1	1	1	0	0	0	0	0	0	1	1	0	1	1	1	1	0	1	0	10	4
32	50	m	1	1	1	1	1	1	1	1	1	1	1	1	1	0	0	1	1	1	1	1	1	0	0	0	0	17	8
33	73	m	1	0	0	1	1	1	1	1	1	0	1	1	1	1	1	1	1	1	1	1	1	1	1	0	0	18	8
34	75	f	1	0	0	1	1	1	1	1	1	1	1	1	1	1	1	1	1	0	0	1	1	0	1	0	0	16	7
35	54	f	0	0	0	1	1	1	1	1	1	1	1	1	1	0	1	1	1	1	1	1	1	0	0	0	0	15	7
36	74	m	1	1	0	1	1	1	1	1	1	1	1	1	0	0	0	1	1	0	0	1	1	0	0	0	0	13	5
37	59	m	1	0	0	1	1	1	1	1	1	1	1	1	1	0	0	0	1	1	0	1	1	1	0	0	0	14	5
38	66	m	1	0	0	1	1	1	1	1	1	1	1	1	0	0	0	1	1	0	0	1	1	0	0	0	0	12	5
39	53	m	1	0	0	1	1	1	1	1	1	1	1	1	1	0	0	1	1	1	1	1	1	0	0	0	0	15	7
40	78	f	1	1	1	1	1	1	1	1	1	0	1	0	0	1	1	1	1	1	1	1	1	1	1	0	0	18	8
																											Minimum	9	4
																											Maximum	18	8
																											Median	13	6

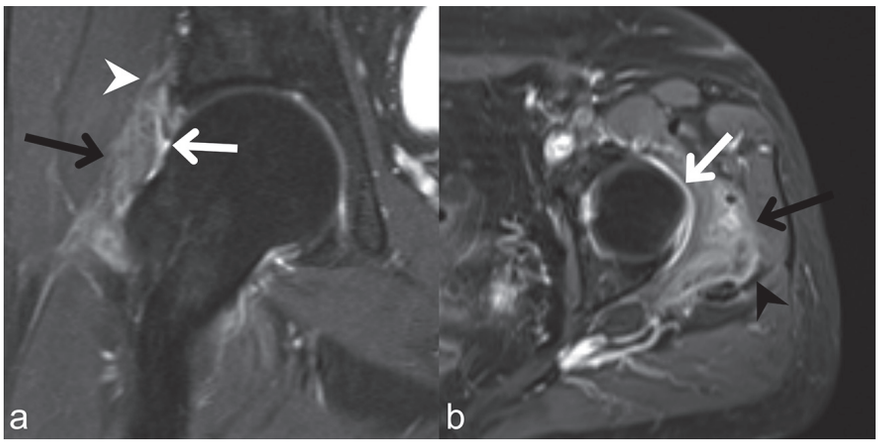

Fig. 5. Coronal (a) and transverse (b) ceT1w FS in two patients. Inflammation of the fibrous capsule of the hip joint and around it (black arrow) is clearly differentiable from synovitis (white arrow). The inflammation merges with peritendinous inflammation of adjacent structures like reflected head rectus femoris (**a**: white arrowhead) or gluteus medius tendon (**b**: black arrowhead).

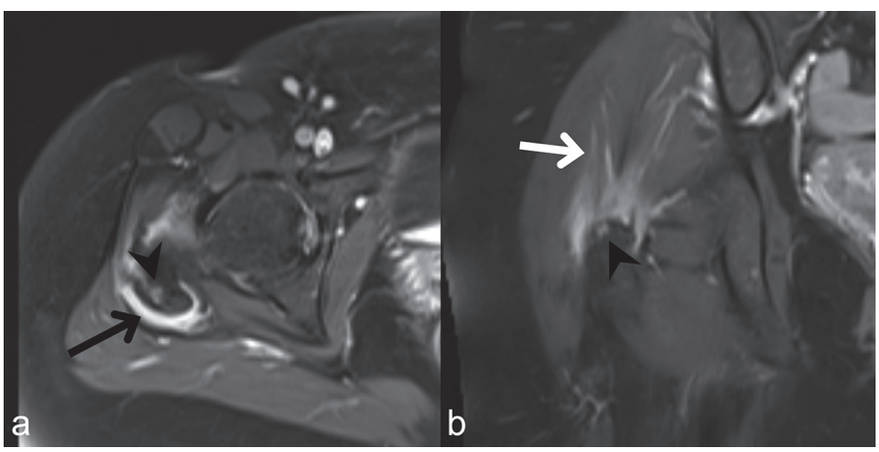

Fig. 6. Transverse (a) and coronal (b) ceT1w FS in same patient. Besides strong trochanteric bursitis between gluteus medius tendon and greater trochanter (**a**: black arrow) there is peritendinous inflammation of gluteus medius tendon up to the myotendinous junction (**b**: white arrow) and minute osteitis of greater trochanter (**a/b**, black arrow head).

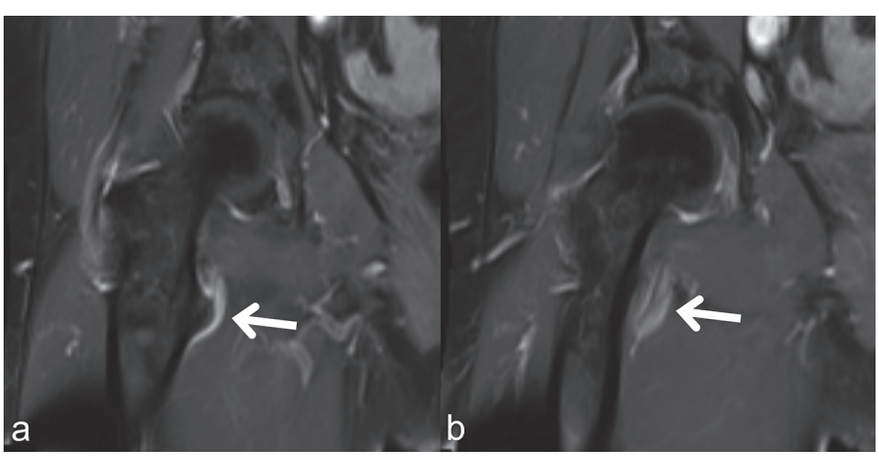

Fig. 7. Coronal ceT1w FS in same patient. Ill-defined peritendinous inflammation of distal iliopsoas tendon directly (**a**) and proximate (**b**) at lesser trochanter (white arrows).

were available for all cases identified on the basis of an expert diagnosis of PMR made between April 2014 and December 2017. The main indication for the MRI examination was the open differential diagnosis. Retrospectively, all patients fulfilled the Bird criteria for PMR of 1979 (17).

The median (25^{th}/75^{th} percentiles) age of the patients was 67 (range 55–73) years, the median symptom duration was 13 (range 6–22) weeks, 55% were female, the median C-reactive protein measured close to the day of the MRI examination was 1.9 (range 0.7–4) mg/dl, and the median erythrocyte sedimentation rate was 30 (range 17–43) after the 1^{st} hour. Only 3 patients were rheumatoid factor positive, of whom one had additionally anti-CCP antibodies and one patient had anti-CCP antibodies but was negative for rheumatoid factor. Ten patients had a diagnosis of RA (25%) in addition to the leading symptom suggestive of PMR.

Magnetic resonance imaging

All patients had undergone a routine pelvic MRI with weight adapted, intravenous applied contrast after written consent. 36 patients were examined with Siemens Aera, 2 patients each with Siemens Skyra and Siemens Avanto. Scanning parameters are given in Table I. The main indication for the scan were differential diagnostic considerations for pelvic girdle pain.

Investigated sites and image analysis

Evaluation of contrast-enhancement around the predefined structures was made for all patients by one musculoskeletal radiologist (MF) on a PACS workstation. Based on our own previous experiences sites of interest were predefined:

- the lumbar interspinous bursae and paraspinous origins of autochthon spinal musculature (SPINE),
- around the superior anterior iliac spine and anterior iliac crest representing various muscle origins like the abdominal wall musculature, including M. tensor fasciae latae and M. sartorius (ASIS),
- around the proximal origin of the straight and reflected head of the tendon of the M. rectus femoris at the anterior inferior iliac spine and supraacetabular ridge (RF),
- around the distal part of the M. glutaeus medius and minimus tendon at the trochanteric insertion (TRO),

- around the fibrous hip capsule at the level of the femoral neck (CAP),
- around the tendon of the M. iliopsoas at the level of the hip joint (IPH),
- around the tendon of the M. obturator internus at its reflection at the posterior margin of os ischium (OBT),
- around the adductor tendon origins at the inferomedial pubic symphysis (SYM),
- around the distal iliopsoas tendon at the lesser trochanter (IPT),
- around the common ischiocrural origin (hamstring) at the ischial tuberosity (IC),
- around the distal insertional site of the M. glutaeus maximus at the gluteal tuberosity (MAX),
- the synovial layer (synovitis) of the hip joints (SYNO).

To be scored positive contrast-enhancement at these sites, it was necessary that two contiguous slices in one plane or on two perpendicular planes were visible. All sites were scored binary, "0" representing no significant enhancement, "1" significant enhancement disrespect individual severity. Additionally, the absence, "0", or presence, "1", of osteitis at insertional sites and myositis were investigated and documented in a similar manner.

Due to different ranges and positioning of the routine pelvic scans some sites could not be assessed. Those sites were scored as "0", this applied to the sites SPINE and ASIS at the cranial and MAX at the caudal border.

Synovitis of hip joints was presumed a secondary feature and is listed but not added to the individual scores. The scoring results are presented in tabular form and superimposed on a hip x-ray.

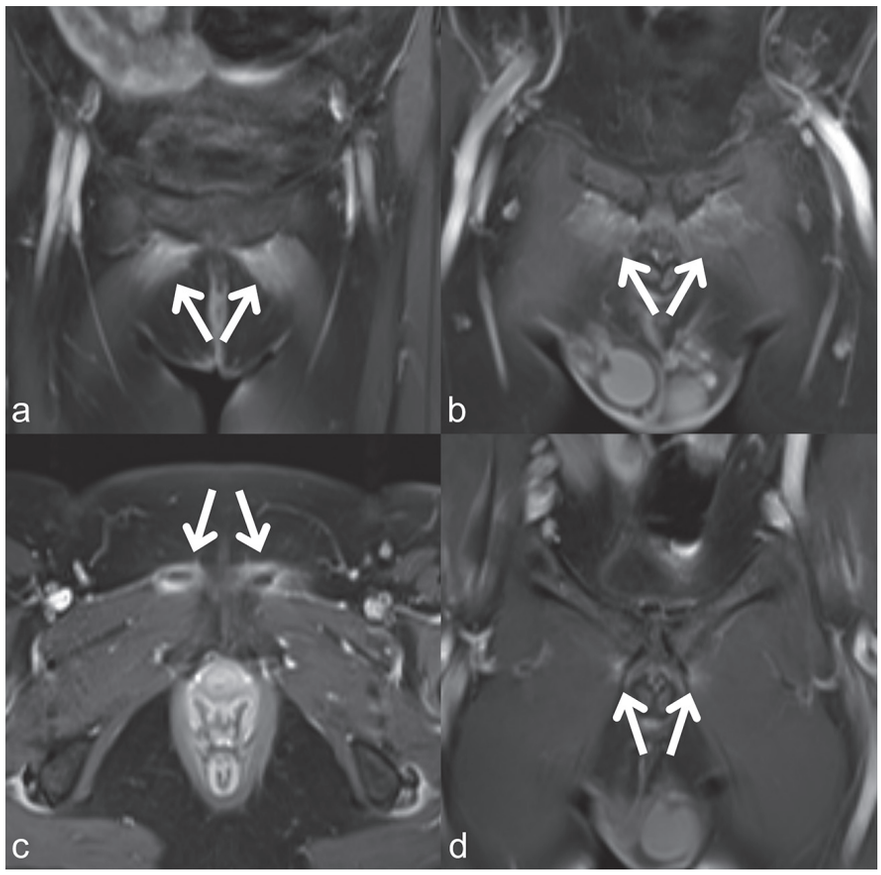

Fig. 8. Coronal and transverse ceT1w FS in two patients. Diffuse intra- and peritendinous inflammation of most inferomedial adductorial origins, mainly adductor longus, in a female (**a/c**) and male (**b/d**) patient (white arrows). In the male patient the inflammation extended posteriorly to adductor brevis and gracilis origin (**d**).

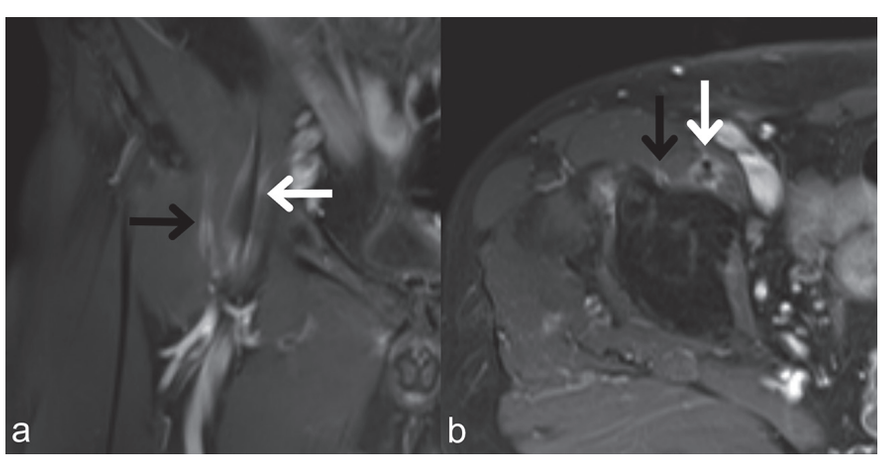

Fig. 9. Coronal and transverse ceT1w FS in same patient. Diffuse peritendinous inflammation around iliacus (black arrow) and psoas (white arrow) at level of hip joint. The aspect of long-segment circumferential inflammation is different from what can be encountered in bursitis.

Results

The typical and common feature observed at all tendinous sites was a uniform peri- and intratendinous enhancement after application of the contrast agent. The spatial degree of enhancement varied from discrete circumferential spots to a strong involvement of the whole tendon up to the myotendinous junction, an example is shown in Figure 1. A pictorial overview of all sites is given in Figures 1-3 and 5-14.

At two sites, a relatively small amount of osteitis at insertional sites was encountered, one at the greater trochanter and one at the pubic bone near the symphysis. In two cases, the peritendinous enhancement extended into the M. glutaeus maximus mimicking myositis. An elevation of the serum creatine kinase (CK) level was, however, absent in both, see Figure 2.

Interestingly, no isolated synovial inflammation was detected – neither near the joints nor the bursae. However, low grade bilateral articular synovial inflammation of the hip joints was a com-

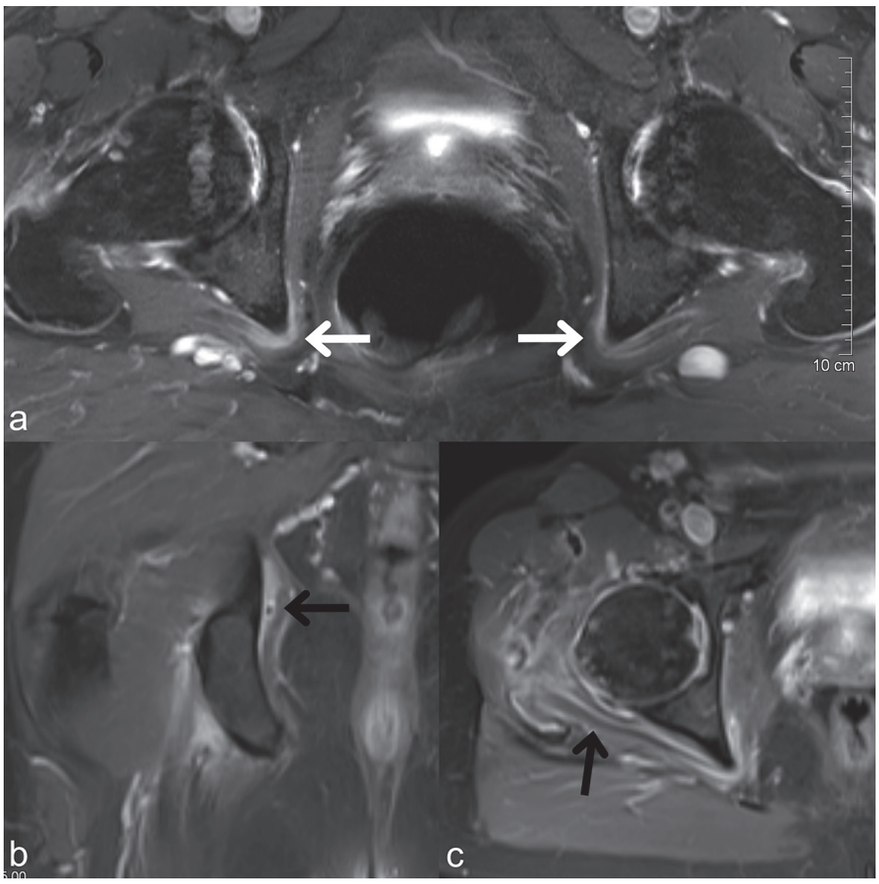

Fig. 10. Transverse and coronal ceT1w FS in two patients. Bilateral peritendinous inflammation of obturator internus tendon around its reflection at ischium (**a**: white arrow) at level of hip joint. In second case (**b**/**c**) unilateral right sided inflammation follows the tendon to the trochanteric fossa and merges with capsular and gluteal tendon inflammation (**c**: black arrow).

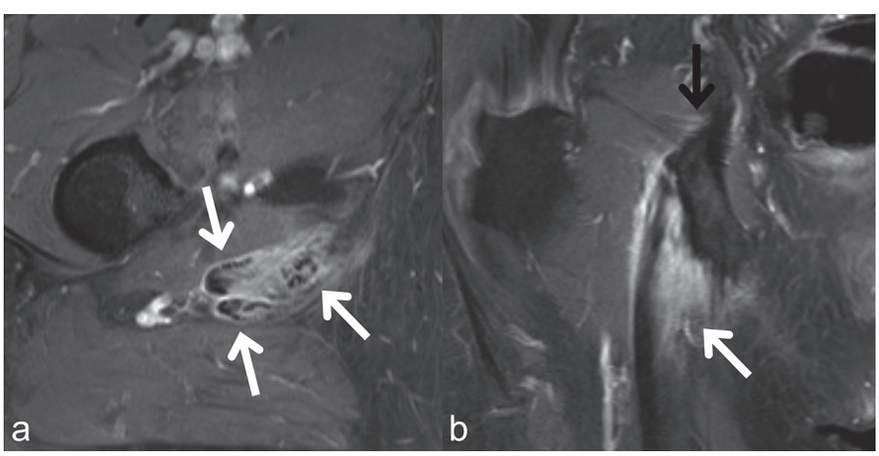

Fig. 11. Transverse and coronal ceT1w FS in same patient. Circumferential and intratendinous inflammation of hamstring tendon, the three tendons (semimembranosus, semitendinosus and biceps femoris) are already separated at level of lesser trochanter (**a**/**b**, white arrows). Note the minute inflammation of obturator internus tendon at ischial reflection (**b**: black arrow).

mon finding that was observed in 35 of 40 cases. An accompanying bursal inflammation at insertions and reflection points was frequently observed, especially at the greater trochanter. However, it was frequently difficult to differentiate this feature from the usually predominant peritendinous enhancement. In 5 cases only extracapsular peritendinous inflammation was detected but no significant synovitis of the hip joints, see Figure 3.

Both the peritendinous enhancement at individual sites and distributional patterns were largely uniform. The consistent radiological feature in all cases was the mostly bilateral enhancement of extracapsular tendinous structures. Bilateral involvement of at least 4 extracapsular sites was the minimal extent of inflammation observed in 6 cases whereas the maximal bilateral involvement was of 8 out of 10 potential sites. The median was 6 sites. The frequency of extracapsular involvement apart from its often-bilateral appearance was also remarkable, with a minimum of 9 affected sites in all cases, and up to 18 affected sites in 8 cases and 13 sites in median, see Table II.

The most frequently affected sites, importantly in all cases bilaterally, were the hamstring tendon (IC), the M. gluteus medius and minimus at the greater trochanter (TRO), and the M. rectus femoris (RF). The adductorial origins at the inferomedial pubic symphysis were affected bilaterally in 90%, paraspinous inflammation and interspinous bursitis (SPINE) in 70%, bilateral inflammation of the distal tendon of the M. iliopsoas (IPT) in 58% and pericapsular inflammation of the fibrous hip capsule (CAP) in 50% of the cases, also see Figure 4.

The underrepresentation of enhancement in sites at the most cranial and caudal borders such as SPINE, ASIS and MAX is at least partially caused by exclusion of those sites due to different scan ranges and consequently scoring as absence of enhancement. Involvement of iliacus and psoas tendon at the level of the hip joint (IPH) was the most challenging assessment hindered by pulsation artefacts of femoral vessels and sometimes difficult to differentiate from pericapsular enhancement of the hip joint. The most frequently inflamed sites, RF, TRO, IC and SYM, were often as well those with the highest individual inflammatory burden.

Based on the semiquantitative scoring we performed in all 40 patients with a confirmed clinical diagnosis of PMR we postulate that bilateral inflammation of the proximal rectus femoris origin and/or the adductorial origin at the inferomedial symphysis pubis with at least 3 other extracapsular sites affected

bilaterally can serve as a positive test to confirm a clinical diagnosis of PMR.

Discussion

In this retrospective analysis of a case series of 40 patients with PMR and available pelvic MRIs, we report a rather specific pattern of involvement of entheseal structures in patients with PMR, by providing evidence of an MRI patho-anatomy that documents predominant inflammation in extracapsular structures. We would like to emphasise that we do not claim that this is a new finding, because others have published several case series showing similar changes with different methods (8-13). However, this is the first time that, based on our relatively large cohort, we make a straightforward claim that the described changes could become a diagnostic tool for PMR.

A recent meta-analysis concluded that subacromial-subdeltoid bursitis is the most helpful ultrasound feature for a diagnosis of PMR (7). Aside from ultrasonographic data, the many reports on imaging features in PMR have been based on FDG-PET/CT (8-13). The whole-body PET-CT scan gives an excellent panoramic view of inflamed sites based on the increased local glucose metabolism. However, the downside is that the PET- component lacks spatial resolution, while the CT-component has poor contrast resolution. Thus, this method provides limited information on the patho-anatomy of the disease. However, this does not argue against its use for diagnostic purposes. Of course, the radiation exposure needs to be taken into account.

In our study, we show that the local site of inflammation is in fact the outer lining of the tendinous and capsular structures, which most likely correspond to the peritendineum externum and internum that continues into the perimysium – which may explain the perimysial inflammation observed in two cases. Since isolated synovial inflammation without accompanying peritendinous or pericapsular inflammation was not detected, synovitis (bursal or articular) seems to just be a non-obligatory secondary phenomenon. In contrast, we did detect extracapsular inflammation without synovitis of the hip joints in 5 cases. Of interest, hypertrophic synovitis as seen in rheumatoid arthritis was not observed at all.

Hardly any osteitis was detected at entheseal sites, similar to an earlier observation by others (14). The involvement of several tendon origins and insertions may well be considered as an expression of a systemic enthesitic disease such as in spondyloarthritides (18), especially in psoriatic arthritis (19), although the low burden of osteitis is rather atypical for a classic enthesitic

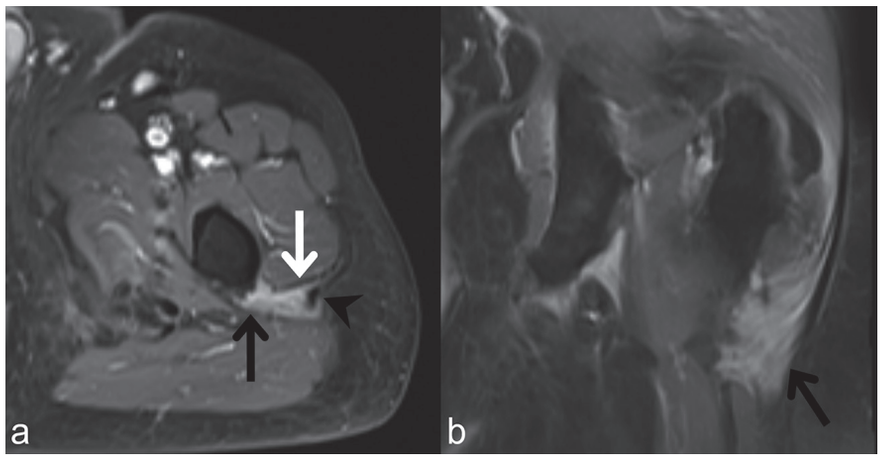

Fig. 12. Transverse and coronal ceT1w FS in same patient. Broad inflammation of distal gluteus maximus insertion at gluteal tuberosity (a/b, black arrow) involves other local fibrous structures like lateral intermuscular septum (a, white arrow) and connection to iliotibial (a, black arrow head).

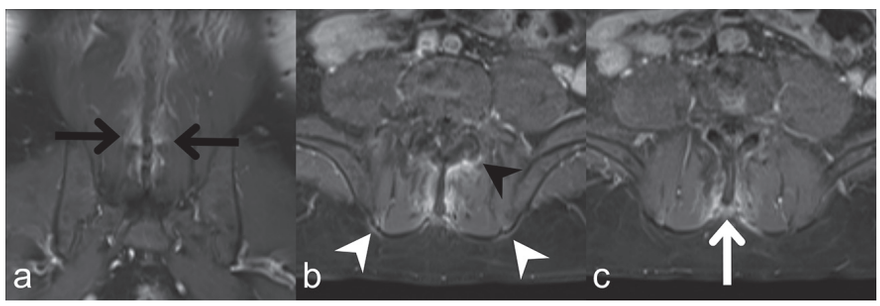

Fig. 13. Coronal and transverse ceT1w FS in same patient. Inflammation affects the direct surrounding of lumbar spinous processes at level L3-L5 representing myoosseous origins of autochthon spinal muscles (a, black arrows). The inflammation extends pericapsular to the left facet joint (b, black arrow head). The thoracolumbar fascia is affected at spinous insertion respective supraspinal ligament (c, white arrow) and lateral at a conjunction with an intermuscular septum (b, white arrow heads).

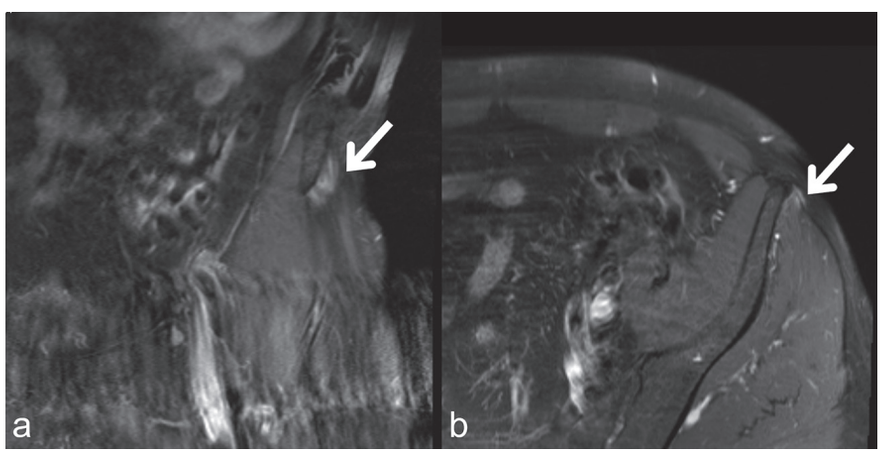

Fig. 14. Transverse and coronal ceT1w FS in same patient. Minute perifascial inflammation at insertion of gluteal fascia at anterior iliac crest (a/b white arrow).

disease spectrum such as spondyloarthritis (20). Therefore, the denomination "enthesitic inflammation" as proposed in earlier PET-CT studies (8, 10) is, in our opinion, not correct. Based on what we have learned from the many MR images studied, we think that the inflammatory process that is frequently observed in PMR targets a structure within the peritendineum, a tissue that contains many blood vessels and neural structures, rather than the enthesis. Of course, the ultimate proof for the precise localisation of the inflammation in PMR must come from histological studies. Such studies also will help to potentially identify a common pathophysiologic basis of GCA and PMR, and hence solve the question whether these can be considered two distinct diseases or only different features of one disease.

The clinical differentiation between PMR and other diseases presenting with polymyalgic pain is currently based on exclusion of other diseases such as vasculitides and malignancy, since a specific diagnostic test for PMR is not available to date. Prospective studies with controls of patients with other diseases are needed to recognise whether our findings will fill the gap of a finding specific for PMR. Our data appear to provide a basis for performing these types of studies, and we do plan to start a prospective trial to answer this question.

The uniform distributional pattern of tendinous inflammation on contrast-enhanced MRI of the pelvis found in PMR patients in this study seems to be specific for PMR. A comparable pattern of inflammation – without accompanying osteitis – does, to the best of our knowledge and in contrast to a recent review (16) not occur in other diseases, including the spondyloarthritides. Based on the semiquantitative scoring we performed in all patients with a confirmed clinical diagnosis of PMR we postulate that bilateral inflammation of the proximal rectus femoris origin and/or the adductorial origin at the inferomedial symphysis pubis with at least 3 other extracapsular sites affected bilaterally can serve as a positive test to confirm a clinical diagnosis of PMR.

The strengths of this study are the relatively high number of cases and the very detailed reading, scoring and documentation performed by an experienced musculoskeletal radiologist in close collaboration with experienced clinicians. Furthermore, the results of the MRI did not influence the clinical diagnosis, because this knowledge was not available at the time the MRIs had been performed.

However, our study also has some limitations which should be addressed before our results can be generalised and proposed for clinical utilisation. We also cannot exclude that the indication for performing the MRI in the first place has led to a non-intended selection for more severe cases. It is possible that patients with milder disease may not show the same changes presented here. Furthermore, we cannot say anything about PMR patients with predominant myalgic neck and shoulder pain – which appears likely to also be characterised a rather specific pattern. Similarly, we can not really say anything on possible differences between 'pure' PMR and cases of RA which initially show a PMR-like pattern or about other vasculitides or malignancy which can also display PMR-like, in that case paraneoplastic symptoms (21, 22). Finally, the analysed MRI scans featured different sequence parameters, varying scan ranges and occasionally slight motion artefacts. However, since the data presented here were compiled from evaluations by one single reader, this study is not appropriate to generalise the findings. Thus, as already mentioned, prospective randomised controlled studies will have to be performed to compare these findings with other diseases, to analyse intra- and interrater reliability, and perform longitudinal analyses of the response to therapy with a control.

Conclusion

We found a uniform pelvic inflammatory pattern in contrast-enhanced MRI in patients who have PMR, an observation that could be applicable as a feasible, specific, diagnostic imaging test. We propose that the bilateral involvement of at least 4 extracapsular sites (including the origins of the rectus femoris or adductorial muscle tendons near symphysis) can serve as a characteristic sign for PMR. Further analyses of specificity and interrater reliability appear needed to better characterise this possible proposed diagnostic imaging test.

References

1. BUTTGEREIT F, DEJACO C, MATTESON EL, DASGUPTA B: Polymyalgia rheumatica and giant cell arteritis: a systematic review. *JAMA* 2016; 315: 2442-58.
2. OZEN G, INANC N, UNAL AU *et al*.: Assessment of the new 2012 EULAR/ACR clinical classification criteria for polymyalgia rheumatica: a prospective multicenter study. *J Rheumatol* 2016; 43: 893-900.
3. DEJACO C, DUFTNER C, BUTTGEREIT F, MATTESON EL, DASGUPTA B: The spectrum of giant cell arteritis and polymyalgia rheumatica: revisiting the concept of the disease. *Rheumatology* (Oxford) 2017; 56: 506-15.
4. DASGUPTA B, CIMMINO MA, MARADIT-KREMERS H *et al*.: 2012 provisional classification criteria for polymyalgia rheumatica: a European League Against Rheumatism/American College of Rheumatology collaborative initiative. *Ann Rheum Dis* 2012; 71: 484-92.
5. DEJACO C, SINGH YP, PEREL P *et al*.: 2015 Recommendations for the management of polymyalgia rheumatica: a European League Against Rheumatism/American College of Rheumatology collaborative initiative. *Ann Rheum Dis* 2015; 74: 1799-807.
6. DEJACO C, RAMIRO S, DUFTNER C *et al*.: EULAR recommendations for the use of imaging in large vessel vasculitis in clinical practice. *Ann Rheum Dis* 2018; 77: 636-43.
7. MACKIE SL, KODURI G, HILL CL *et al*.: Accuracy of musculoskeletal imaging for the diagnosis of polymyalgia rheumatica: systematic review. *RMD Open* 2015; 1: e000100.
8. WAKURA D, KOTANI T, TAKEUCHI T *et al*.: Differentiation between polymyalgia rheumatica (PMR) and elderly-onset rheumatoid arthritis using 18F-fluorodeoxyglucose positron emission tomography/computed tomography: is enthesitis a new pathological lesion in PMR? *PLoS One* 2016; 11: e0158509.
9. SONDAG M, GUILLOT X, VERHOEVEN F *et al*.: Utility of 18F-fluoro-dexoxyglucose positron emission tomography for the diagnosis of polymyalgia rheumatica: a controlled study. *Rheumatology* (Oxford) 2016; 55: 1452-7.
10. REHAK Z, SPRLAKOVA-PUKOVA A, BORTLICEK Z *et al*.: PET/CT imaging in polymyalgia rheumatica: praepubic 18F-FDG uptake correlates with pectineus and adductor longus muscles enthesitis and with tenosynovitis. *Radiol Oncol* 2017; 51: 8-14.
11. OWEN CE, POON AMT, LEE ST *et al*.: Fusion of positron emission tomography/computed tomography with magnetic resonance imaging reveals hamstring peritendonitis in polymyalgia rheumatica. *Rheumatology* (Oxford) 2018; 57: 345-53.
12. KUBOTA K, YAMASHITA H, MIMORI A: Clinical value of FDG-PET/CT for the evaluation

of rheumatic diseases: rheumatoid arthritis, polymyalgia rheumatica, and relapsing polychondritis. *Semin Nucl Med* 2017; 47: 408-24.
13. REHAK Z, SPRLAKOVA-PUKOVA A, KAZDA T, FOJTIK Z, VARGOVA L, NEMEC P: 18F-FDG PET/CT in polymyalgia rheumatica-a pictorial review. *Br J Radiol* 2017; 90: 20170198.
14. MACKIE SL, PEASE CT, FUKUBA E *et al*.: Whole-body MRI of patients with polymyalgia rheumatica identifies a distinct subset with complete patient-reported response to glucocorticoids. *Ann Rheum Dis* 2015; 74: 2188-92.
15. OCHI J, NOZAKI T, OKADA M *et al*.: MRI findings of the shoulder and hip joint in patients with polymyalgia rheumatica. *Mod Rheumatol* 2015; 25: 761-7.
16. BUTTGEREIT F, MATTESON EL: Imaging: Whole-body MRI undresses polymyalgia rheumatica. *Nat Rev Rheumatol* 2016; 12: 140-1.
17. BIRD HA, ESSELINCKX W, DIXON AS, MOWAT AG, WOOD PH: An evaluation of criteria for polymyalgia rheumatica. *Ann Rheum Dis* 1979; 38: 434-9.
18. BARALIAKOS X, KILTZ U, APPEL H *et al*.: Chronic but not inflammatory changes at the Achilles' tendon differentiate patients with peripheral spondyloarthritis from other diagnoses - Results from a prospective clinical trial. *RMD Open* 2017; 3: e000541.
19. TAN AL, MCGONAGLE D: Psoriatic arthritis: correlation between imaging and pathology. *Joint Bone Spine* 2010; 77: 206-11.
20. SCHETT G, LORIES RJ, D'AGOSTINO MA *et al*.: Enthesitis: from pathophysiology to treatment. *Nat Rev Rheumatol* 2017; 13: 731-41.
21. MULLER S, HIDER SL, BELCHER J, HELLIWELL T, MALLEN CD: Is cancer associated with polymyalgia rheumatica? A cohort study in the General Practice Research Database. *Ann Rheum Dis* 2014; 73: 1769-73.
22. UNGPRASERT P, SANGUANKEO A, UPALA S, KNIGHT EL: Risk of malignancy in patients with giant cell arteritis and polymyalgia rheumatica: a systematic review and meta-analysis. *Semin Arthritis Rheum* 2014; 44: 366-70.